Eur. Phys. J. D **41**, 303–309 (2007)
DOI: 10.1140/epjd/e2006-00218-8

THE EUROPEAN PHYSICAL JOURNAL D

# Characterization of the ion cathode fall region in relation to the growth rate in plasma sputter deposition

A. Palmero[a], E.D. van Hattum, H. Rudolph, and F.H.P.M. Habraken

Surfaces, Interfaces and Devices, Department of Physics & Astronomy, Utrecht University, P.O. Box 80.000, 3508TA Utrecht, The Netherlands

Received 19 May 2006
Published online 27 September 2006 – 

**Abstract.** In plasma-assisted magnetron sputtering, the ion cathode fall region is the part of the plasma where the DC electric field and ion current evolve from zero to their maximum values at the cathode. These quantities are straightforwardly related to the deposition rate of the sputtered material. In this work we derive simple relations for the measurable axially averaged values of the ion density and the ion current at the ion cathode fall region and relate them with the deposition rate. These relations have been tested experimentally in the case of an argon plasma in a magnetron sputtering system devoted to depositing amorphous silicon. Using a movable Langmuir probe, the profiles of the plasma potential and ion density were measured along an axis perpendicularly to the cathode and in front of the so-called race-track. The deposition rate of silicon, under different conditions of pressure and input power, has been found to compare well with those determined with the relations derived.

**PACS.** 52.77.-j Plasma applications – 52.77.Dq Plasma-based ion implantation and deposition – 81.15.Cd Deposition by sputtering

## 1 Introduction

Plasma-assisted sputter deposition is one of the most widely used techniques to grow thin films [1–3]. The scientific challenge in the understanding of the strongly non-linear plasma sputtering deposition process is in the combination of several different fields like surface and plasma physics (see for instance [4–7] and references therein). In general, sputtering systems contain a cathode through which electromagnetic power is coupled into a reactor containing an inert gas. In the plasma positive ions are created, mainly in the cathode fall region, and accelerated towards the cathode. The ions hit the cathode with an energy of several hundreds eV and sputter on average several atoms per incoming ion. Some of the sputtered atoms reach a grounded substrate, stick on the surface and hence contribute to the growth of the layer. Essentially this describes the basic steps in the plasma sputtering deposition.

There are many valuable ongoing efforts to describe the distinct steps of the plasma deposition on a more fundamental level (see for instance [8,9] and references therein), but in the present work we attempt to describe and understand the entire process of deposition using a semi-empirical approach. We are stimulated by the following question: which of the many measurable, possibly relevant, and non-linearly related plasma quantities, apart from the externally adjustable parameters, do we need to determine in order to predict the deposition rate in a particular plasma deposition system? The suggestion from this work is that, by using only one measurable plasma quantity, we can eliminate all system-dependent influences, like the system geometry, the magnetic field configuration and the location where the gases flow into the system. The predictions following from the relations found in this paper are compared with measurements of the spatially resolved ion density and the ion cathode fall thickness, as determined with a Langmuir probe under various experimental conditions. In addition, we have determined the deposition rate using Elastic Recoil Detection (ERD). Using these measurements we have found a satisfying agreement with the predictions.

The paper is organized as follows: in the following section we describe the theoretical approach. In Section 3 we describe the experimental set-up, whereas in Section 4 we present and discuss the experimental results. Finally in Section 5 we summarize the conclusions.

## 2 Theoretical approach

The sputtering rate, $r_s$, which we define as the number of atoms sputtered per unit of area and unit of time is given by the relation

$$r_s = Y J_i \tag{1}$$

[a] e-mail: a.palmeroacebedo@phys.uu.nl

where $Y$ is the sputtering yield, i.e., the average number of sputtered atoms per incident ion for perpendicular incidence [10]. The value of $Y$depends on the nature of the ions, their energy, and the structure and composition of the cathode material. $J_i$ is the ion current density at the cathode. When the mean free path of the sputtered particles is larger than the distance between the cathode and the film, the sputtering rate is proportional to the deposition rate, $r_d$, and hence the ratio $r_d/r_s$ is constant. The main difficulty here is, that $J_i$ is a quantity which is not straightforward to determine experimentally under general conditions. For this reason we try to relate the current density to other parameters that are easier to measure.

In the cathode fall region, with thickness $D$, defined as the region from the cathode to the place in the plasma bulk where the DC electric field strength is zero, we distinguish two regions: (i) the pre-sheath, typically several centimetres length, characterized by its quasi-neutrality and by a small value of the electric field strength, and (ii) the sheath, typically several millimetres length, in which the electron density is negligible compared to the ion density and in which the electric field strength is large.

The theoretical description of the ion cathode fall region is in general difficult. However, in the sheath region a relation between the ion current in the plasma and the potential fall can be derived under simple assumptions [11]:

$$J_i = \frac{4\varepsilon_0}{9}\left(\frac{2}{em_i}\right)^{1/2}\frac{(\Delta V_{sh})^{3/2}}{d^2}, \tag{2}$$

where $\Delta V_{sh}$ is the measured DC potential fall in the sheath, $d$ its thickness, $e$ the electron charge, $m_i$ the ion mass, and $\varepsilon_0$ the electrical permittivity in vacuum. Equation (2) is commonly known as the Child-Langmuir law, and has been found applicable for RF discharges [12,13] and for magnetron plasmas in the sheath created in front of the so-called race-track [14]. The main difficulty when using equation (2) from an experimental point of view, however, is the determination of $d$. In reference [15] it was concluded that in RF plasmas, $d$ weakly depends on the input electromagnetic power used to maintain the discharge, and that it depends on the gas pressure, $p$, as $d \propto p^n$, where $n$ is an exponent depending on the composition of the plasma.

The thickness of the cathode fall region, $D$, is easier to determine experimentally than $d$. From a practical point of view it would be useful to have a description that allows the characterization of the ion transport towards the cathode based on $D$, instead of $d$. This is part of the strategy of the present work. Due to the complexity of the plasma discharge it will appear necessary to make rough approximations to achieve this. It is not the goal of this paper to accurately describe the plasma detailed in space and in time.

The typical extent of the pre-sheath depends strongly on the collisional aspects of the ions in the plasma. If the ions are in a strongly collisional regime, it is related to the ion mean free path. In a weakly collisional regime, where the ions suffer, on average, few collisions on their way from the plasma bulk towards the cathode, the thickness of the pre-sheath and of the sheath has been theoretically found to scale as

$$\begin{aligned} d &\propto \lambda_D, \\ D &\propto d^{4/5}\lambda_{ia}^{1/5}, \end{aligned} \tag{3}$$

$\lambda_D$ is the so-called Debye length, and $\lambda_{ia}$ the mean free path for elastic and charge-exchange collisions between ions and neutral atoms [16]. These laws were experimentally found to be valid [17].

We consider a one-dimensional, one-species, low ionized steady-state plasma where the ions are in a weakly collisional regime. The input electromagnetic signal may oscillate in time, but we will assume that the ions are accelerated towards the cathode on a time scale much longer than the period of the electromagnetic wave, and their movement can therefore be described by the DC component, i.e., the time averaged value of the electric field. $z$ is the axial coordinate, where $z = 0$ is the position of the cathode, and $z = D$ is the position where the DC electric field component is zero.

We consider the Poisson's law

$$\frac{\partial^2 V(z,t)}{\partial z^2} = -\frac{e}{\varepsilon_0}\left[n_i(z) - n_e(z,t)\right], \tag{4}$$

where $n_e$and $n_i$ is the electron and ion density, respectively, and $V$ the electric potential, related to the electric field, $E$, through $E(z,t) = -\partial V(z,t)/\partial z$. Integrating twice between $z = 0$ and $z = D$ in equation (4) we find

$$V(0,t) = V(D,t) + DE(D,t) - \frac{e}{\varepsilon_0}\int_0^D dy\int_y^D dz\left[n_i(z) - n_e(z,t)\right].$$

Averaging in time, over one period of the electromagnetic signal, and taking into account that $\langle E(D,t)\rangle = 0$, where $\langle\ \rangle$ refers to one-cycle averaged values, we find

$$\Delta V \propto D^2\left(\overline{n_i} - \overline{n_e}\right), \tag{5}$$

with $\Delta V = \langle V(0,t)\rangle - \langle V(D,t)\rangle$, and with $\overline{n_i}$ and $\overline{n_e}$ defined as

$$\overline{n_i} = \frac{2}{D^2}\int_0^D dy\int_y^D dz\, n_i(z),$$

and

$$\overline{n_e} = \frac{2}{D^2}\int_0^D dy\int_y^D dz\,\langle n_e(z,t)\rangle. \tag{6}$$

The values of $\overline{n_i}$ and $\overline{n_e}$ can be considered as the two-dimensional spatially averaged electron and ion density, respectively, in a right triangular domain with side $D$. These definitions contrast the commonly used 1-dimensional average: for the ion density for instance $\overline{n_i^{1-dim}} = (1/D)\int_0^D dz\, n_i(z)$. However, if the axial profile

of the densities is smooth enough along most of the cathode fall region, the 1-dimensional and the 2-dimensional averages should show the same behaviour when changing the deposition conditions. For this reason, we will refer to them as the spatially averaged values of the ion and electron density.

To continue our description we will make rough estimations in order to find the general trends of the plasma quantities. In general, the pre-sheath of the plasma can be considered quasi-neutral on average, i.e. $\langle n_e(z,t)\rangle = n_i(z)$ for $d < z \leq D$, whereas the electron density can be considered negligible in the plasma sheath. In this case, using equation (6) we approximate

$$\overline{n_e} = \frac{2}{D^2}\int_d^D dy \int_y^D dz\, n_i(z) \simeq \overline{n_i}\frac{(D-d)^2}{D^2} \simeq \overline{n_i}\left(1-\frac{2d}{D}\right), \tag{7}$$

where in the last step we have made a Taylor's expansion to the first order since $d \ll D$. Besides, we have also assumed that the profile of the ion density in the cathode fall region is smooth enough to assume that the spatially averaged value of the ion density in the pre-sheath is a good estimation of the spatially averaged ion density in the whole cathode fall. Using equations (5) and (7) we find the relation $\overline{n_i} \propto \Delta V/Dd$. Using equation (3), and knowing that $\lambda_{ia} \propto 1/p$, we finally obtain

$$\overline{n_i} \propto \frac{\Delta V}{D^{9/4}p^{1/4}}. \tag{8}$$

In addition, the ion current at the cathode is given by equation (2), i.e., $J_i \propto (\Delta V_{sh})^{3/2}/d^2$. By knowing that the potential fall along the pre-sheath is in the order of several volts, and that the potential fall in the sheath is in the order of hundreds of volts, we approximate $\Delta V \simeq \Delta V_{sh}$, thus using equation (3) again, we obtain

$$J_i \propto \frac{(\Delta V)^{3/2}}{D^{5/2}p^{1/2}}. \tag{9}$$

Equation (9) is especially important, since $\Delta V$ and $p$ are usually experimentally known and, hence, any technique that provides the changes in $D$, by using an appropriate calibration, therefore allows the determination of the ion current density in the plasma, and thus the deposition rate in the system by using equation (1). In addition, $D$ and $\overline{n_i}$ are related through equation (8), thus, any measurement that yields the trend of the spatially averaged ion density under varying deposition conditions would make it possible to determine the deposition rate, after an appropriate calibration.

## 3 Experimental set-up

The deposition system is contained within a vacuum vessel with a base pressure of $10^{-5}$ Pa. The cathode (target), made of poly-crystalline silicon, is circular and has an area of $7.9\times10^{-3}$ m$^2$. It is powered with a 13.56 MHz RF voltage, and a ring of permanent magnets is surrounding a single magnet with reversed polarity placed in the center behind the target (with respect to the plasma). The average magnetic field strength near the cathode is estimated to be 0.05 T. The one-cycle averaged electric potential of the cathode is monitored by the power supply.

The distance between the cathode and the anode (deposition surface) amounts to 8.5 cm. The anode has a hole with a diameter of 15 mm. This hole enables a Langmuir probe to be inserted into the plasma perpendicularly to the cathode. The entire cathode can be moved up/down by means of an electrical manipulator connected to the top of the vessel, permitting a spatially resolved plasma characterization. The experimentally adjustable quantities in this system are the deposition pressure and the input RF power. The cathode potential, as monitored by the power supply, varied only slightly with pressure under typical deposition conditions. For more details about the experimental set-up see references [18,19].

The technique used to obtain the plasma quantities with the Langmuir probe in a non-zero magnetic field intensity has previously been explained in reference [18]. Values of the ion density and the plasma potential were determined in front of the race-track, i.e., where the magnetic field is parallel to the cathode and perpendicular to the ion current. The racetrack is the region where the most intense sputtering takes place, and it is therefore the most interesting region to study the plasma-cathode interaction. The silicon deposition rate was measured using the high-energy-ion beam technique ERD, which yields accurately values for the areal density of elements in the surface layers. Further details concerning the application of this technique in the present situation can be found in reference [19].

## 4 Results and discussion

In Figure 1 we present the plasma potential profile, measured with a Langmuir probe, for an input RF power of 100 W, and for various gas pressures. We can clearly discern two important spatial regions: starting from the part of the plasma further away from the cathode, we see the plasma bulk with an increasing electric potential when we approach the cathode. Here, the electric field points towards the deposited film, making all the ions in this region move towards it. This part of the plasma is commonly known as the negative glow region. As we get closer to the cathode, the plasma potential starts to become constant until it reaches a maximum towards the ion cathode fall region. The distance between the cathode and this maximum of the plasma potential defines $D$. In Figure 2 it is shown that we find similar profiles in the plasma potential for a gas pressure of 0.67 Pa, and for different input RF powers. The results presented in Figures 1 and 2 agree quite well with those presented in reference [18], where the values of the plasma potential, determined with the Langmuir probe, were confirmed with an energy-resolved mass spectrometer.

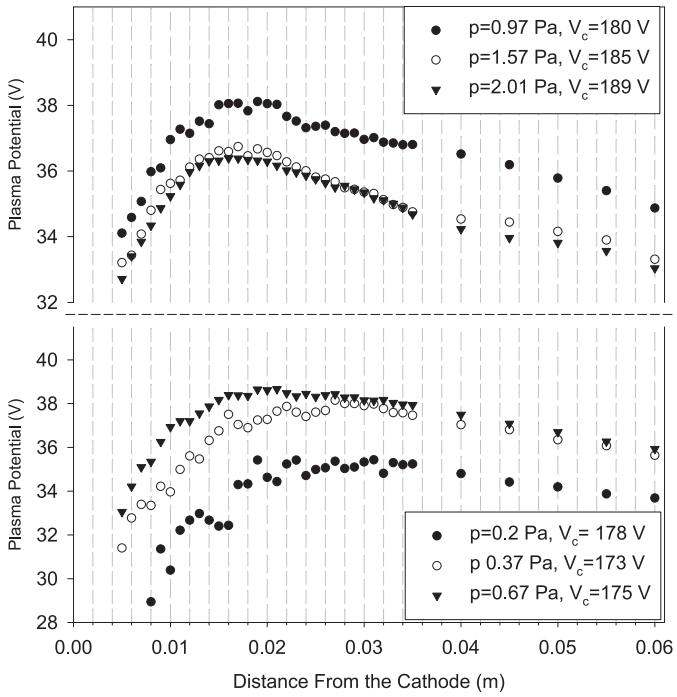


**Fig. 1.** Plasma potential as a function of the distance to the cathode for different gas pressures. The RF input power amounted always to 100 W. The bottom part contains the lower pressure measurements and the top part the higher pressure measurements. Statistical error of the data is below 5%.

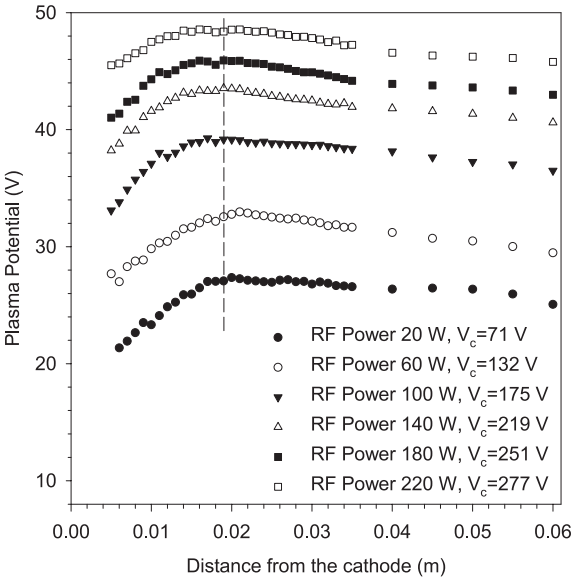


**Fig. 2.** Plasma potential as a function of the distance to the cathode for different input RF powers. The gas pressure always amounted to 0.67 Pa. The dashed line points to the fact that $D$ is weakly dependent on the value of the RF input power. Statistical error of the data is below 5%.

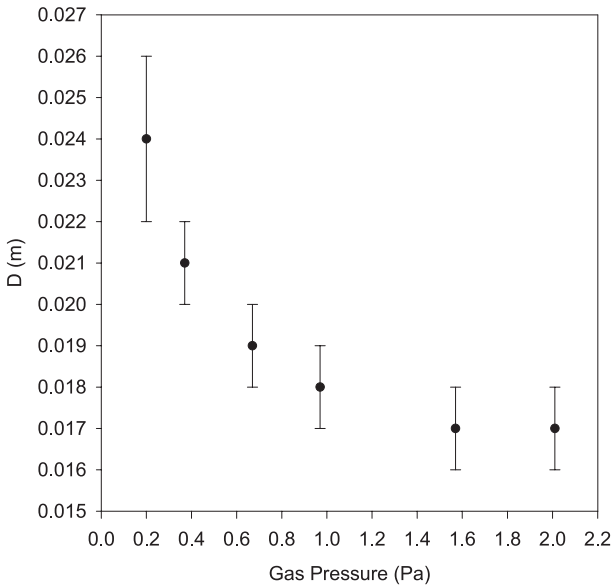


**Fig. 3.** Plasma cathode fall thickness as a function of the gas pressure, estimated from Figure 1.

In Figure 3 we present the value of $D$ for the gas pressures under the same conditions as in Figure 1. As seen in Figure 2, the value of $D(\simeq 0.02$ m) is not very sensitive to changes in the power, but it increases significantly towards lower pressures. These trends agree with the results presented in reference [15]. The next step, in order to check the relations presented in equations (8, 9), is to find whether the experimental conditions presented in Figures 1 and 2 correspond to a weakly collisional regime for the argon ions. This condition is achieved when

$$\frac{m_i v_i \frac{dv_i}{dx}}{m_i v_i \nu_{ia}} \sim \frac{\lambda_{ia}}{D} \sim 1.$$

The cross section for ion/atom elastic and resonant charge exchange collisions is estimated to be $\sigma_{ia} \simeq 9.3 \times 10^{-19}$ m$^2$ [20], and therefore $\lambda_{ia}/D \simeq 0.2/p$ (Pa). For gas pressures around 0.2 Pa, we are therefore in the weakly collisional regime for the ions.

In Figure 4a we present the ion density as a function of the distance from the cathode for different gas pressures under the same conditions as in Figure 1. These values agree quite well with those obtained in reference [17]. The ion density increases with pressure, and increases when getting closer to the cathode, both in the bulk and in the plasma pre-sheath. In Figure 4b we present the value of $\Delta V/p^{1/4}D^{9/4}$ and the spatially averaged ion density in the pre-sheath obtained from Figure 4a. Furthermore, in Figures 5a and 5b we show the behavior of the ion density with input RF power and the spatially averaged ion densities, respectively. Equation (8) clearly describes the behavior of the spatially averaged ion density in the cathode fall region as a function of pressure and incident RF power, except for a gas pressure of 0.2 Pa in Figure 4b. This disagreement is most likely due to the lack of sufficient data available for the ion population next to the cathode. This is due to the presence of a thicker plasma sheath that modified the current collected by the Langmuir probe, which makes it difficult to determine the ion population in this region when the probe penetrates it.

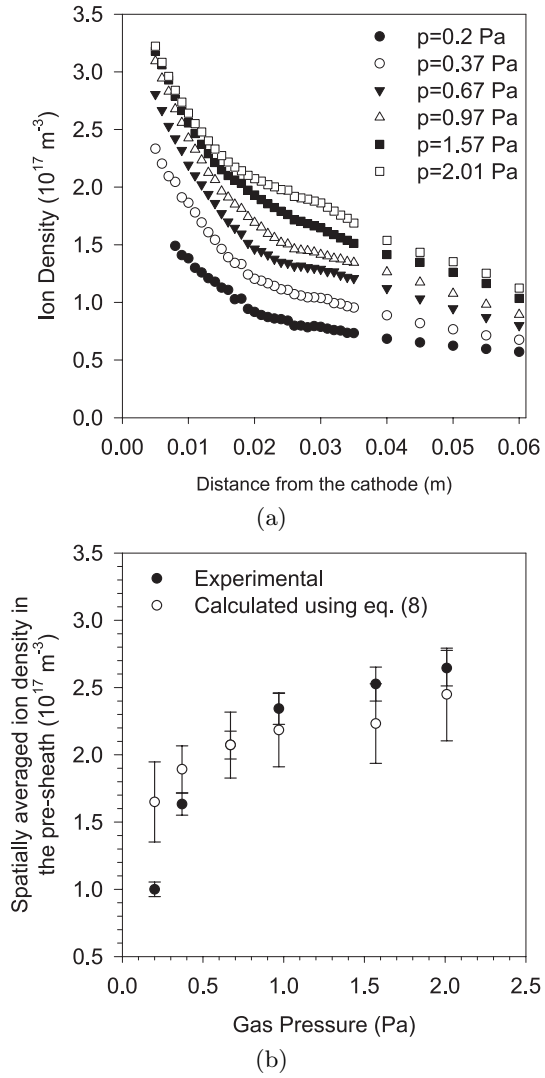


**Fig. 4.** Ion density at different gas pressures, under the same conditions as Figure 1. (a) As measured (statistical error of the data below 5%), and (b) spatially averaged ion density in the pre-sheath, from (a), and calculated using equation (8). Data were fitted at a gas pressure of 0.67 Pa.

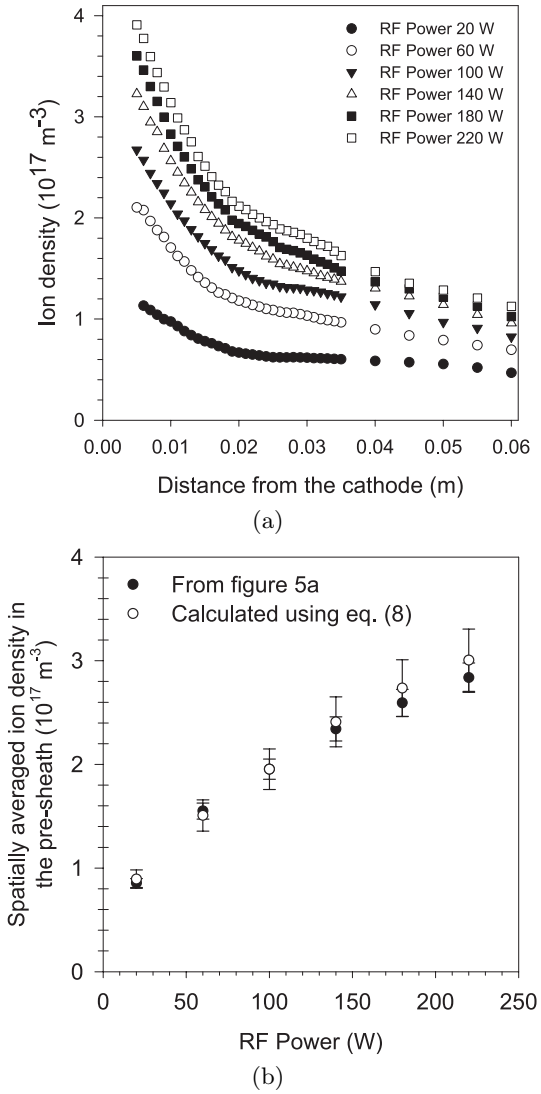


**Fig. 5.** Ion density at different RF input powers, in the same conditions than Figure 2. (a) As measured (statistical error of the data below 5%), and (b) spatially averaged ion density in the pre-sheath, from (a), and calculated using equation (8). Data were fitted at a RF power of 100 W.

The deposition rate under low-pressure conditions can be approximated in a simple manner as $r_d \propto r_s \propto YJ_i$. For higher pressures this relation is not so straightforward, since the sputtered particles have a significant amount of collisions with the background gas, and a part of the sputtered atoms is not deposited onto the anode. At these higher pressures, the well-known Keller-Simmons formula, which relates the sputtering rate and the deposition rate, has to be applied [21]. For silicon sputtering by argon ions, the simple proportionality between $r_d$ and $r_t$ is valid when the gas pressure is below the value $p_0d_0/L$, where $L$ is the distance between the cathode and the film and $p_0d_0$ the so-called thrown distance ($p_0d_0 = 0.081$ Pa m for argon sputtering of silicon) [22], and hence in our system, for gas pressures below approximately 1 Pa. In our case we can therefore simply relate the plasma current and the deposition rate for pressures below that threshold by knowing the dependence of the sputtering yield on the ion energy.

In Figure 6 we present the experimentally determined silicon sputtering yield dependence on the ion energy, $\varepsilon_i$, in the case of a silicon cathode bombarded by argon ions at a normal incidence [23]. In the low energy range (i.e., below approximately 300 eV), the dependence of the sputtering yield can be described by $Y \propto (\varepsilon_i - \varepsilon_t)$, where $\varepsilon_t$ is the sputtering threshold. After performing a fit in the low energy region we have found the value $\varepsilon_t = 31$ eV. For higher energies (i.e. above 300 V) we fit the dependence with $Y \propto \sqrt{\varepsilon_i}$.

The argon ions are accelerated towards the cathode in the pre-sheath and the sheath regions. However, the main acceleration takes place in the plasma sheath where the electric field greatly increases, and whose thickness

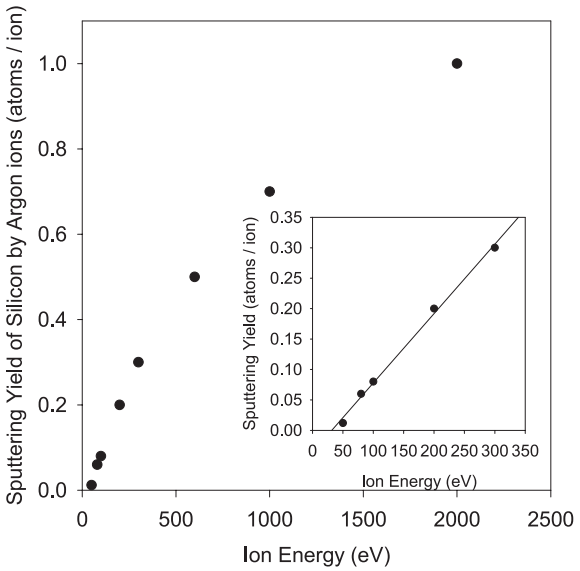


**Fig. 6.** Sputtering yield of silicon by argon ions as a function of the ion energy. The insert presents the same results for the low energy range. The data are reproduced from reference [23].

is much smaller than that of the pre-sheath. As a consequence, collisions are not expected in the sheath in the range of pressures presented in this paper, and therefore the ion kinetic energy will be preserved. Again, using the fact that the potential fall in the pre-sheath is in the order of the electron temperature [16], i.e., much lower than the potential fall in the sheath, we can approximate the energy of an ion when hitting the cathode by $\varepsilon_i \approx e\Delta V$.

Based on equation (9) and the data presented in Figure 6 we deduce the following equations for the sputtering rate

$$r_s \propto \begin{cases} \dfrac{(\Delta V)^{3/2}(\Delta V - V_t)}{D^2 (pD)^{1/2}} & \Delta V \leq 300 \text{ V}, \\ \dfrac{(\Delta V)^2}{D^2 (pD)^{1/2}} & \Delta V > 300 \text{ V}, \end{cases} \quad (10)$$

with $V_t = \varepsilon_t / e$. Under the conditions presented in this paper, $\Delta V$ is always below 300 V.

In Figure 7a we present the deposition rate as a function of the pressure, measured using ERD, and the values obtained through equation (10). In general, the agreement is fairly good, and these relations predict the general trend of the deposition rate as a function of pressure in the range between 0.2 and 1 Pa. It is remarkable here that despite the fact that $D$ depends on pressure, the rest of the terms in equation (10) compensate such changes, resulting in an almost constant deposition rate, which agrees with the experimental trend we have found. In Figure 7b we show the deposition rate for a constant gas pressure and different input RF powers, along with the trends given by equation (10). From Figures 7a and 7b we can conclude that the behavior of the deposition rate can be characterized by equation (10) when changing the input RF power or deposition pressure.

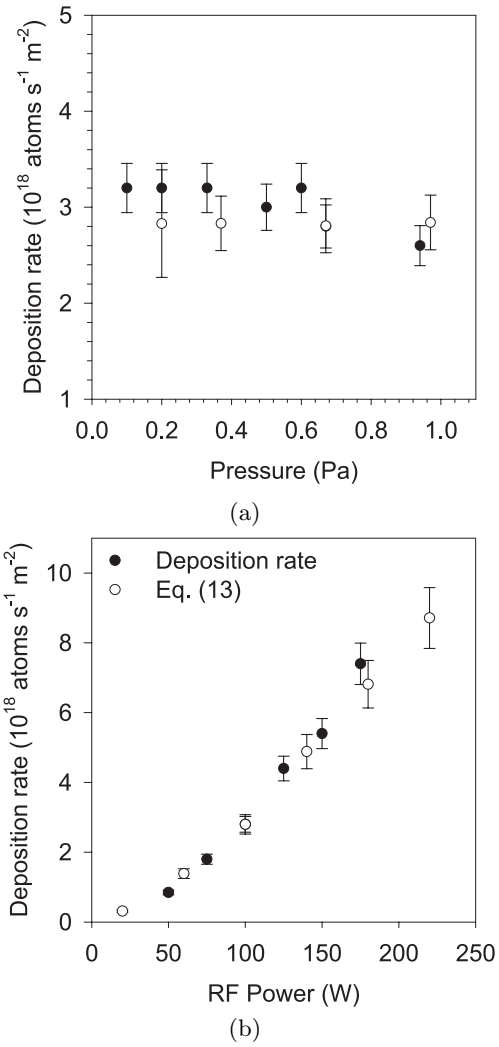


**Fig. 7.** Deposition rate of silicon measured using ERD, and the trend given by equation (10), (a) for RF input power of 100 W and different gas pressures. The calculated data and the deposition rate were fitted at a gas pressure of 0.67 Pa, (b) for a gas pressure of 0.67 Pa and different input RF powers. The calculated data and the deposition rate were fitted at a RF power of 100 W.

The relations given in equations (8, 9), and the results presented in Figures 4b, 5b and 7a and 7b are applicable under many scientifically and technologically important plasma conditions. The implications are obvious: if certain experimentally adjustable quantities are known, such as the gas pressure and the potential fall at the cathode, and one plasma quantity such as $D$, the deposition rate in the system can be determined, after proper calibration and knowledge of the sputtering yield.

Equation (8) allows the estimation of the trend of $D$ by knowing the value of $\overline{n_i}$. This could allow the development of a probe-based mechanism to measure $\overline{n_i}$ near the cathode, and thereby monitor the overall deposition process. This probe can easily be a non-intrusive relatively cheap method based on for instance optical emission spectroscopy, whose applicability will be studied in the future.

## 5 Conclusions

We have found general relations between the plasma quantities in the ion cathode fall region in a sputtering plasma. These relations connects the ion cathode fall thickness, the spatial averaged ion density and ion current at the cathode, which allows to determine the deposition rate of the film. These relations have been experimentally tested in case of an argon plasma in an RF magnetron sputtering system devoted to deposit amorphous silicon layers. Using a Langmuir probe, the profiles of the plasma potential and the ion density in front of the so-called race-track have been measured, as well as the deposition rate of silicon under different pressure and input RF power conditions. The experimental trends compare relatively well with predictions based on the relations presented in this paper.

We would like to acknowledge OCE Technologies, Venlo (The Netherlands) for the support given to this work.

## References

1. R.D. Arnell, P.J. Kelly, Surf. Coat. Technol **112**, 170 (1999)
2. B. Window, Surf. Coat. Technol. **81**, 92 (1996)
3. J. Musil, J. Vlcek, Surf. Coat. Technol **112**, 162 (1999)
4. E.D. van Hattum, A. Palmero, W.M. Arnoldbik, F.H.P.M. Habraken, Surf. Coat. Technol. **188-189**, 399 (2004)
5. J.W. Bradley, M. Cecconello, Vacuum **49**, 315 (1998)
6. S. Berg, T. Nyberg, H.O. Blom, C. Nender, J. Vac. Sci. Technol. A **16**, 1277 (1998)
7. J. Musil, J. Vlcek, Surf. Coat. Technol. **112**, 162 (1999)
8. I. Kolev, A. Bogaerts, Plasmas Proc. Polymers **3**, 127 (2006)
9. B.F. Gordiets, J.L. Andujar, C. Corbella, E. Bertran, Eur. Phys. J. D **35**, 505 (2005)
10. K. Wasa, S. Hayakawa, *Handbook of Sputter Deposition Technology* (Noyes Publications, 1992), p. 61
11. F.F. Chen, *Introduction to Plasma Physics* (Plenum press, 1974), p. 244
12. C. Chang, Z.J. Jin, C. Whitaker, J. Appl. Phys. **62**, 1633 (1987)
13. J.B. Kim, K. Kawamura, Y.W. Choi, M.D. Bowden, K. Muraoka, IEEE. Trans. Plas. Sci. **27**, 1510 (1999)
14. M.L. Escrivao, P.J.S. Pereira, M.H. Cabral, M.R. Teixeira, J.P. Maneira, J. Vac. Sci. Technol. A **21**, 375 (2003)
15. N. Mutsukura, Y. Fukasawa, Y. Machi, T. Kubota, J. Vac. Sci. Technol. A **12**, 3126 (1994)
16. K.-U Riemann, Phys. Plasmas, **4**, 4158 (1997)
17. L. Oksuz, N. Hershkowitz, Phys. Rev. Lett. **89**, 145001 (2002)
18. A. Palmero, E.D. van Hattum, W.M. Arnoldbik, F.H.P.M. Habraken, J. Appl. Phys. **95**, 7611 (2004)
19. E.D. van Hattum, W.M. Arnoldbik, A. Palmero, F.H.P.M. Habraken, Thin Solid Films **494**, 13 (2006)
20. J.R. Roth, *Industrial Plasma Engineering*, Vol. 2: Applications to Nonthermal Plasma Processing (Institute of Physics Publishing, 2001), p. 245
21. A. Palmero, H. Rudolph, F.H.P.M. Habraken, Appl. Phys. Lett. **87**, 071501 (2005)
22. T.P. Drüsedau, M. Löhmann, B. Garke, J. Vac. Sci. Technol. A **16**, 2728 (1998)
23. K. Wittmaack, Phys. Rev. B **68**, 235211 (2003)